Theoretical study on the electronic structure, formation and absorption spectra of lithium, sodium and potassium complexes of N-confused tetraphenylporphyrin

ARTICLE *in* COMPUTATIONAL AND THEORETICAL CHEMISTRY · SEPTEMBER 2013

Impact Factor: 1.55 · DOI: 10.1016/j.comptc.2013.07.014

3 AUTHORS, INCLUDING:

Demeter Tzeli
National Hellenic Research Foundation
52 PUBLICATIONS **502** CITATIONS
SEE PROFILE

Ioannis D Petsalakis
National Hellenic Research Foundation
142 PUBLICATIONS **1,590** CITATIONS
SEE PROFILE

Computational and Theoretical Chemistry 1020 (2013) 38–50

Contents lists available at SciVerse ScienceDirect

Computational and Theoretical Chemistry

journal homepage: www.elsevier.com/locate/comptc

Theoretical study on the electronic structure, formation and absorption spectra of lithium, sodium and potassium complexes of N-confused tetraphenylporphyrin

Demeter Tzeli *, Ioannis D. Petsalakis, Giannoula Theodorakopoulos

Theoretical and Physical Chemistry Institute, National Hellenic Research Foundation, 48 Vassileos Constantinou, Athens 116 35, Greece

ARTICLE INFO

Article history:
Received 16 January 2013
Received in revised form 4 June 2013
Accepted 10 July 2013
Available online 19 July 2013

Keywords:
N-confused porphyrin
Complexes
Na
K
Li
Calculations

ABSTRACT

The present work is a theoretical study on lithium, sodium and potassium complexes of N-confused tetraphenylporphyrin (NCTPP). Its purpose is to determine the stability, binding, absorption spectra and formation energy of the complexes of NCTPP with sodium and potassium, studied here for the first time. All calculations were carried out employing density functional theory (DFT) and time-dependent DFT, using the B3LYP, PBE0 and M06-2X functionals in conjunction with the 6-31G(d,p) basis set. The results show that the energy ordering of different low-lying minimum energy structures of the three metal complexes is not the same, with the global minimum energy structures of the lithium and sodium resulting from the same tautomer of NCTPP while potassium complexes result from another tautomer of NCTPP. The insertion of Li, Na and K into NCTPP in the presence of THF is exothermic with reaction energies calculated to be −68, −56 and −50 kcal/mol using the corresponding metal bis-(trimethylsilyl)amide reagents. The absorption vis–UV spectra are similar for the different metals and the Q and Soret bands are slightly red shifted as the metal changes from Li to K.

1. Introduction

N-confused porphyrins (NCPs) are porphyrin isomers having one pyrrole ring inverted, resulting in three nitrogen atoms and one carbon atom at the macrocycle core and the inverted nitrogen atom at the β-position on the periphery of the macrocycle, cf. Scheme 1. Since their first syntheses [1] singly and doubly NCPs, i.e., with one and two inverted pyrrole groups, have been studied extensively [2–5]. They form a variety of stable organometallic compounds displaying multimodal coordination properties [2,3]. In addition, the peripheral nitrogen atom (of the inverted pyrrole ring) can act as a hydrogen bonding donor or acceptor, resulting in the formation of multiporphyrin systems [3] As a result, NCPs are candidates for applications in many areas of chemistry and materials science [3].

Metal complexes of NCPs have been generated using mostly main group elements, lanthanides, and transition metal ions, [2,3,5] while for complexes of group IA with NCPs, there are only two very recent studies, one experimental [6] and one theoretical [7] on lithium complexes of N-confused tetraphenylporphyrin (NCTPP) and its 21-N-methylated variant. Sripothongnak and Ziegler, [6] synthesized and characterized by x-ray diffraction lithium complexes of NCTPP and obtained their absorption spectrum. The theoretical study on the same systems, conducted by our group, was performed employing the DFT theory [7]. The theoretical results confirmed the experimental conclusions for the most part, but a different interpretation was provided regarding the type of metal-porphyrin bonding involved in the complexes. In particular it was found that in these complexes Li does not adopt the typical tetrahedral coordination of Li^+ (eg. found in complexes of Li with porphyrin) [8] but it forms a stronger bond with one of the three available N atoms with a nearly planar coordination [7]. The fact that lithium almost fits in the porphyrin cavity may result in lithium being effectively sequestered [9]. As far as we know, there is no study (experimental or theoretical) on the complexes of any of the remaining group IA metals with NCTPP or any NCPs. Generally, theoretical studies on free-base NCPs [4b,7,10] or metal complexes of NCPs [5f,i,7] are few, while there is a significant number of experimental studies [1–5].

The importance of the alkali metal NCP(M-NCP) arises from the possibility that they be used as synthetic reagents like the alkali metal normal porphyrins (M-P). The latter have been used as synthetic reagents for the preparation of a wide range of M-P (c.f., M = Sc, Zr, and Hf) in high yield (for instance >90% for M = Sc) [11]. In general the stabilities of M-P decreased in the order small divalent > large divalent > alkali metal with some exceptions under specific conditions [11].

* Corresponding author. Tel.: +30 210 7273 813; fax: +30 210 7273 794.
E-mail addresses: dtzeli@eie.gr, idpet@eie.gr (D. Tzeli).

2210-271X/$ - see front matter © 2013 Elsevier B.V. All rights reserved.
http://dx.doi.org/10.1016/j.comptc.2013.07.014

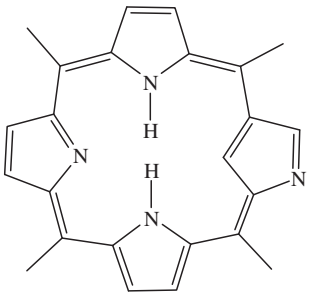

Scheme 1.

In the present work, we study theoretically sodium and potassium complexes of NCTPP employing density functional theory (DFT). We determine the stability and the binding of the above complexes by geometry optimization calculations of the ground electronic state. The excited electronic states and the absorption spectra of their different conformers are calculated. Moreover, additional calculations to our previous study on lithium complexes of NCTPP [7] have been carried out. Our aim is to compare the lithium, sodium and potassium complexes of NCTPP with respect to the stability, the binding and the absorption spectra, and to determine whether Na or K adopt an unusual coordination environment, like that observed in the Li complexes of NCTPP [7]. The final goal is to provide information for the potential use of alkali metal NCP as synthetic reagents like the alkali metal normal porphyrins do.

2. Methods

We calculated seven tautomers of free N-confused tetraphenylporphyrin (NCTPP) (**1a**–**1g**) given in Fig. 1; the sodium and potassium complexes of the three lowest energy of NCTPP, **1a**, **1b**, and **1c** (**1aNa**, **1bNa**, **1cNa**, **1aK**, **1bK** and **1cK**) and the Li complex with the **1c** tautomer (**1cLi**) given in Fig. 2; the sodium and potassium complexes of the two lowest energy of NCTPP, **1a** and **1b** in the presence of one tetrahydrofuran (THF) molecule (**1aNaTHF**, **1bNaTHF**, **1aKTHF**, and **1bKTHF**) given in Fig. 3. The above structures are given in more detailed on Figs. 1S and 2S of the ESM. The calculations were carried out both in the gas phase and in toluene solvent. For all calculated structures shown in Figs. 1–3, the harmonic frequencies were calculated confirming that they are true energy-minima.

For brevity we employ the abbreviation NCTPP for N-confused tetraphenylporphyrin, in both free and complex forms, even though in the complex form, one of the hydrogen atoms of the ligand has been replaced by a metal atom. Since it was found [6] that Li-NCTPP synthesized in 5% anhydrous THF in toluene produced pseudo-five coordinated Li complexes and it would be interesting to address the question whether the corresponding Na and K complexes could be formed, all metal complexes have also been calculated in the presence of one tetrahydrofuran (THF) molecule. Similarly, in normal porphyrins with Li, Na, and K, the metal also forms bond with solvent molecules such as THF or OEt_2 [8]. Only one THF molecule has been included because there is no space for more than one THF molecule to form a complex with M-NCTPP.

In our previous work [7], complexes of the N-confused tetraphenylporphyrin (**1a** and **1b** tautomers) with lithium in the presence or absence of THF were calculated employing the B3LYP [12], CAM-B3LYP [13], and M06-2X [14] functionals in conjunction with the 6-31G(d,p) [15] basis set. All three functionals predicted similar geometries, in agreement with the available crystallographic data, and they yielded similar population analyses. However, it was concluded that the M06-2X functional was more suitable for the calculation of the reaction energies of the Li-NCTPP complexes judging from test calculations on simple systems such as the LiN molecule. The M06-2X/6-31G(d,p) method is in complete agreement with the MRCI/aug-cc-pV5Z_N/cc-pVQZ_{Li} [16] results for the D_e values, while the CAM-B3LYP and B3LYP functionals result in small deviations [7]; nonetheless all three DFT methods are in good agreement with respect to the bond distance of the ab initio method. Additionally, we found that the calculated vis–UV spectra of the conformers are similar using either the M06-2X or the CAM-B3LYP functional, while the corresponding B3LYP peaks are shifted to lower energies, which are in better agreement with experimental values.

Taking into account the conclusions of the previous work on the suitability of the functionals [7], all calculated structures of the present work were fully optimized using the B3LYP [12] and M06-2X [14] functionals in conjunction with the 6-31G(d,p) [15] basis set in the gas phase and in toluene solvent. Additionally, the PBE0 [17] functional was employed to compare its results with

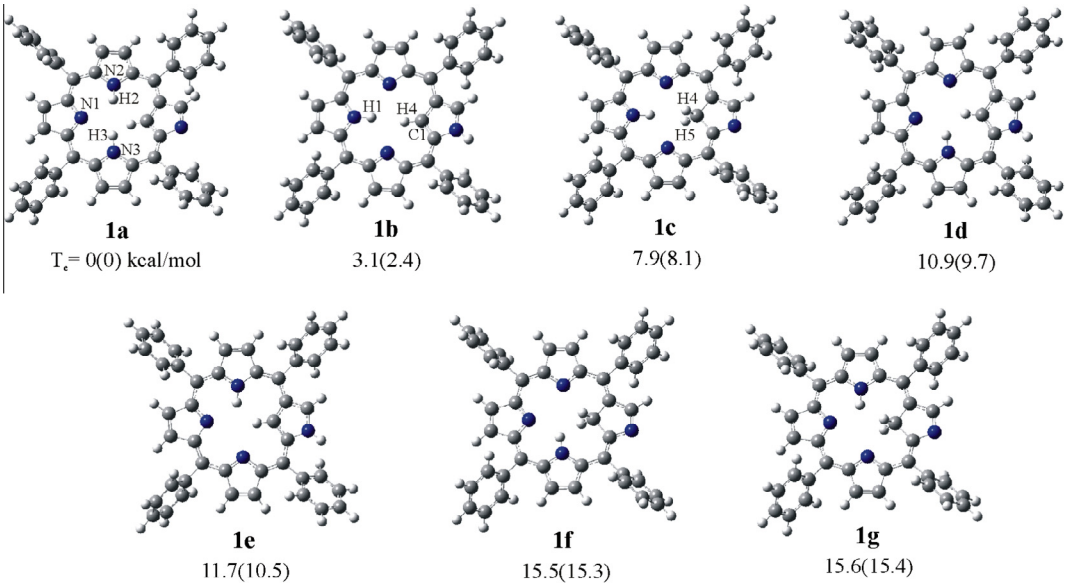

Fig. 1. 1a-1g minima. Energy differences T_e from the most stable structure are shown in the gas phase (in toluene solvent) at the M06-2X/6-31G(d,p) level of theory.

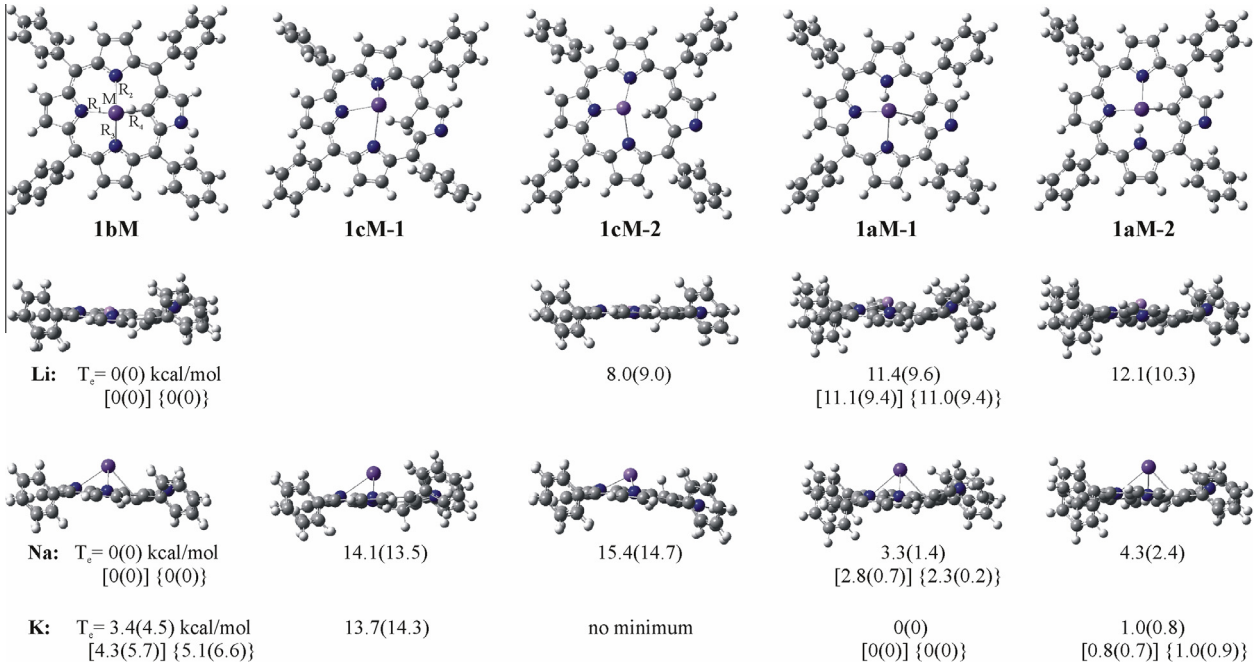

Fig. 2. **1aM**, **1bM**, and **1cM** minima, where M = Li, Na, and K. Energy differences T_e from the most stable structure are shown in the gas phase (in toluene solvent) at the M06-2X[PBE0]{B3LYP}/6-31G(d,p) levels of theory.

the corresponding results of the M06-2X and B3LYP functionals. PBE0 combines the PBE generalized gradient functional with a predefined amount of exact exchange, [17] and it is a reliable functional for the study of excited electronic states of organic molecules, see refs. [18,19] and references therein.

Finally, in order to calculate the reaction energy of the insertion of Na and K to NCTPP, we carried out calculations on the reagents, sodium and potassium bis-(trimethylsilyl) amide and bis-(trimethylsilyl)amine, i.e., $NaN(Si(Me)_3)_2$, $KN(Si(Me)_3)_2$, and $HN(Si(Me)_3)_2$ respectively, at the M06-2X/6-31G(d,p) level of theory.

The polarizable continuum model (PCM) [20] was employed for the inclusion of the toluene solvent. This method is one of the most often used for reliable continuum solvation procedures [21].

The singlet-spin excited electronic states of the separated species and their complexes have been calculated via Time Dependent DFT (TDDFT) [22] in the gas phase and in toluene solvent. The lowest 50 excited electronic states of the complexes have been determined at the optimized ground state geometry, relevant to the absorption spectra in order to calculate the Q, B(Soret), N, L, and M bands [23] and to identify the differences among the absorption spectra of the three metal complexes of NCTPP.

Basis set superposition error (BSSE) corrections have been taken into account using the counterpoise procedure [24] for all studied minima.

All calculations were carried out using the Gaussian 09 program package [25]. The coordinates of all the optimized structures are included in the accompanying Electronic supplementary information (ESM).

3. Results and discussion

3.1. Geometries and bonding

3.1.1. NCTPP

Seven minimum-energy tautomers of the NCTPP molecule (**1a**–**1g**) are shown in Fig. 1. In our previous study on the Li-NCTPP clusters only the two lowest minima **1a** and **1b** were considered [7]; both of which have been observed in solution [1,10] with **1a** the preferred tautomer in aromatic and halogenated solvents and also in the gas phase [1,7,10]. Here, five additional tautomers are calculated to examine whether other minima of the NCTPP molecule can lead to low-lying stable complexes with metals. The third minimum structure of the NCTPP molecule, **1c**, has two hydrogen atoms attached to C1 and lies energetically at 8 kcal/mol above **1a** at the M06-2X/6-31G(d,p) level of theory in toluene solvent. As we show below, **1c** forms low-lying metal complexes. It might be noted that when only one hydrogen atom is connected to one of the N1, N2, or N3 atoms, it prefers to be connected to the N1 atom. As a result, the **1b** minimum is more stable by about 8 kcal/mol than **1d** or **1e** and similarly **1c** is more stable than **1f** or **1g** by about 8 kcal/mol, see Fig. 1.

3.1.2. M-NCTPP

The replacement of one hydrogen atom connected to N atoms (N1, N2 or N3) of the core in the three lowest minimum tautomers **1a**, **1b**, and **1c** of the NCTPP molecule with M = Li, Na, and K results in the M-NCTPP minimum energy structures, i.e., **1aM-1**, **1aM-2**, **1bM**, **1cM-1**, and **1cM-2**, shown in Fig. 2. The **1aLi** and **1bLi** structures [7] are given here for comparison. The **1aM-1** and **1aM-2** minima differ in which hydrogen atom of the free base porphyrin has been replaced, namely H3 and H2, respectively (see Fig. 2). In **1bM**, **1cM-1**, and **1cM-2** the hydrogen atom H1 has been replaced by the metal atom. Structures **1cM-1** and **1cM-2** differ in the relative position of M with respect to H4 and H5 atoms, attached to C1; in **1cM-1** the M atom is placed close to one hydrogen atom of C1, while in **1cM-2** the M atom is placed between the two hydrogen atoms of C1. There are some differences among the **1cM** structures of the three metals. In the case of the Na metal both **1cM-1** and **1cM-2** structures are stable minima. In the case of K only the **1cK-1** structure is stable, because optimization of the **1cK-2** structure results in the **1cK-1** minimum. The situation is reversed for the Li complexes, where **1cLi-1** is not a minimum energy structure and its optimization leads to **1cLi-2**. The **1cLi** structures had not been calculated in our previous study [7]. The energy differences

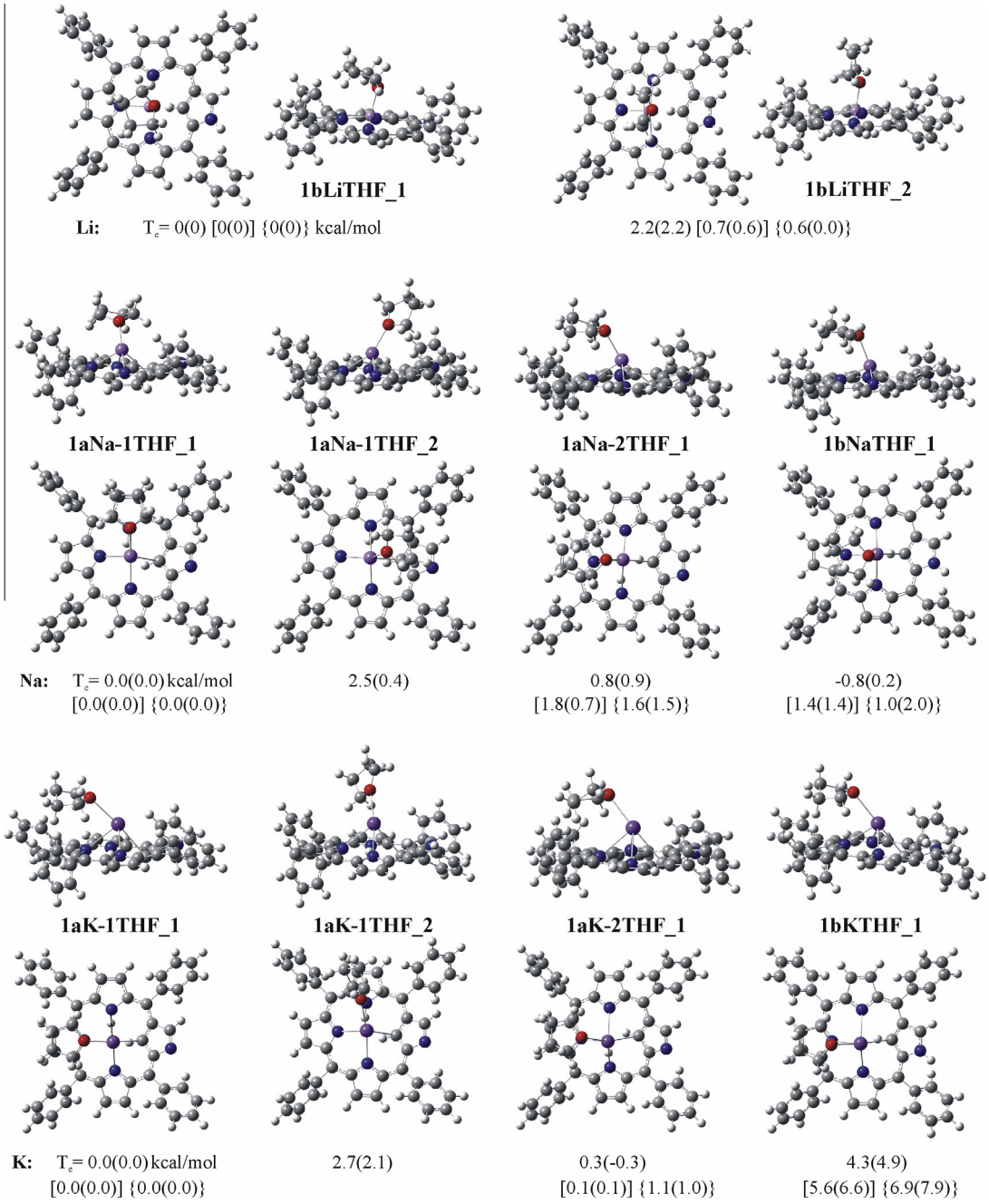

Fig. 3. **1aMTHF** and **1bMTHF** minima, where M = Li, Na, and K. Energy differences T_e from the most stable structure are shown in the gas phase (in toluene solvent) at the M06-2X[PBE0]{B3LYP}/6-31G(d,p) levels of theory.

T_e from the most stable structure for each metal in the gas phase and in toluene solvent at the three levels of theory are also included in Fig. 2.

The relative ordering of the different minimum energy structures of the free NCTPP (H_2NCTPP) and the M-NCTPP complexes for M = Li, Na and K are depicted in Fig. 4. It is very interesting that all three M-NCTPP complexes present different energy ordering. In free NCTPP the ordering is (**1a, 1b, 1c**), in Li-NCTPP complex it changes to (**1b, 1c, 1a**), in Na-NCTPP complex it changes again to (**1b, 1a, 1c**), while in K-NCTPP complex it returns to (**1a, 1b, 1c**) as in the free NCTPP. The reason is that the Li atom is small enough to fit in the porphyrin core but the N–Li bond is larger than the N–H by 0.9 Å; thus Li prefers energetically the **1bLi** structure because only one H atom is connected to the other three core atoms (N or C). Na and K form more elongated N–M bonds. Thus, they do not fit in the core and they are located above it. For these reasons the **1aM** structure is stabilized. While in Li complexes the difference between **1bLi** and **1aLi** is about 11 kcal/mol, in Na complexes their energy difference is reduced to 3 kcal/mol and in K complexes it is reversed to −3 kcal/mol resulting in the **1aK** structure to be the global minimum.

The optimized geometries obtained using the three functionals (B3LYP, M06-2X, PBE0) are similar, see Table 1S of the ESM. Some selected bond lengths obtained using the M06-2X functional in the gas phase and in toluene solvent are given in Table 1. In all **1*n*M** minima, *n* = **a**, **b**, and **c**, the N–M distances ranges from 1.8 to 2.0 Å for the **1*n*Li** minima, 2.2-2.3 for **1*n*Na**, and 2.6-2.7 for **1*n*K**. The smallest N–M distances are observed for the **1cM** minima.

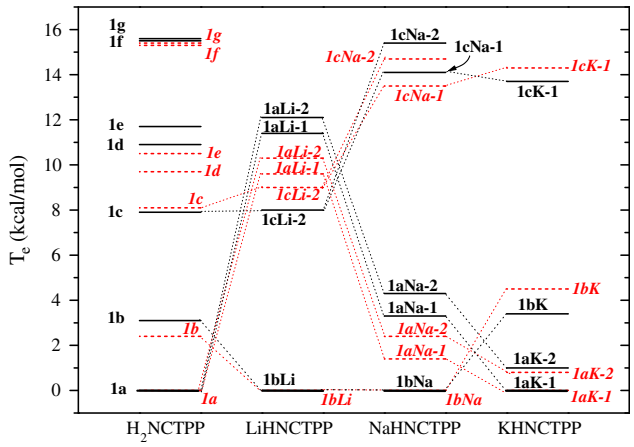

Fig. 4. Relative energy differences of the **1a-1g**, **1aM**, **1bM**, and **1cM** species, where M = Li, Na, and K in the gas phase (black solid lines) and in toluene solvent (red dash lines) at the M06-2X/6-31G(d,p) level of theory.

The distance between the M atom and the plane of the three inner N atoms ranges from 0.03 (**1cLi-2**) to 0.7 (**1aLi-1**) Å for the **1*n*Li** minima, i.e., the **1cLi-2** minimum has the Li atom practically on the plane of the N atoms. The corresponding ranges for the **1*n*Na** and **1*n*K** minima are 0.9–1.2 and 1.6–1.8 Å above the plane, respectively, see Table 1. Comparing the geometries in the gas phase and in solvent we conclude that for the Li complexes the bond lengths are almost the same, while in the cases of Na and K complexes there are some differences. The K complexes present the largest differences up to 0.1 Å, see Table 1. In general, the toluene solvent results in an elongation of the bonds with the exception of the **1cNa** structures.

As mentioned above all minimum energy structures of the M-NCPP have been formed with the replacement of one hydrogen atom connected to N atoms of the free NCTPP. The metal atoms form a bond with these N atoms, and additionally the metal atoms interact and form bonds (less strong, i.e., with elongated bond length) with the remaining two N atoms as well. Moreover, the metal atoms are located in the right place to form an agostic-like interaction with the internal C atom (C1). While, Li complexes are quasi-planar, the Na and K complexes adopt a more typical tetrahedral coordination and the metals are above the porphyrin core. Comparing the present calculated M-NCTPP with other metal-NCPs, e.g., metals that form M^{2+} cations such as Fe [5b,c], Ni [5i], and Zn [5f], two H–N bonds break and the metal cation fits in the NCP cavity with M–N bond lengths of 1.9–2.0 Å, similar to those of the Li-NCTPP where too the Li species fits in the NCTPP cavity.

Table 1
Geometry, R(Å) and φ(degrees) of **1**, **1aM**, **1bM, 1cM**, **1aMTHF**, and **1bMTHF** species in the gas phase and in toluene solvent at the M06-2X/6-31G(d,p) level of theory; crystallographic data are also included.

Species	$R_{M\text{-}N1}$	$R_{M\text{-}N2}$	$R_{M\text{-}N3}$	$R_{M\text{-}d}$[a]	$R_{O\text{-}d}$[a]	$R_{M\text{-}O}$	$R_{M\text{-}C1}$	$R_{M\text{-}H4}$	$R_{C1\text{-}H4}$	φ_{MH4C1}
1bLi[b]	1.909	2.086	2.059	0.230			2.390	1.992	1.078	97.8
[c]	1.916	2.093	2.067	0.267			2.394	2.005	1.079	97.3
Expt.[d]	1.916(6)	2.067(6)	2.085(6)	0.226			2.363(6)	1.981	1.005	99.4(3)
1aLi-1[b]	1.979	2.614	1.927	0.686			2.398	2.078	1.083	93.3
1aLi-2[b]	1.980	1.926	2.616	0.675			2.379	2.057	1.083	93.3
1cLi-2	1.847	2.066	2.057	0.028			2.242	1.831/1.889[e]	1.096	96.7
1bLiTHF_1[b]	1.942	2.125	2.131	0.452	2.426	1.987	2.395	2.048	1.079	94.9
[c]	1.942	2.127	2.134	0.460	2.433	1.985	2.396	2.044	1.079	95.2
Expt.[d]	1.938(4)	2.149(4)	2.156(4)	0.556	2.498	1.983(4)	2.482(4)	2.040	0.957	106.0(2)
1bLiTHF_2[b]	1.943	2.116	2.120	0.417	2.392	1.983	2.398	2.029	1.079	96.2
1bNa	2.220	2.313	2.316	0.926			2.502	2.255	1.079	90.2
[c]	2.244	2.347	2.352	1.018			2.538	2.276	1.079	91.1
1cNa-1	2.263	2.387	2.360	1.126			2.893	2.134	1.078	125.2
[c]	2.241	2.329	2.319	1.010			2.831	2.104	1.079	122.3
1cNa-2	2.178	2.447	2.419	1.208			2.641	2.012	1.095	113.1
[c]	2.144	2.375	2.362	1.080			2.564	1.998	1.098	108.3
1aNa-1	2.307	2.665	2.287	1.231			2.595	2.396	1.081	88.1
[c]	2.342	2.827	2.304	1.376			2.704	2.482	1.080	89.8
1aNa-2	2.301	2.284	2.648	1.214			2.566	2.361	1.080	88.3
1bNaTHF_1	2.249	2.345	2.354	1.018	3.132	2.287	2.536	2.283	1.079	90.7
[c]	2.261	2.362	2.367	1.055	3.164	2.294	2.552	2.289	1.078	91.3
1aNa-1THF_1	2.377	2.932	2.271	1.415	3.200	2.216	2.664	2.521	1.081	85.5
[c]	2.394	3.066	2.291	1.519	2.997	2.227	2.769	2.607	1.080	87.0
1aNa-1THF_2	2.364	2.808	2.296	1.356	3.359	2.237	2.676	2.466	1.080	89.1
[c]	2.395	2.911	2.306	1.446	3.153	2.256	2.745	2.563	1.080	87.9
1aNa-2THF_1	2.363	2.309	2.753	1.314	3.239	2.234	2.645	2.435	1.080	88.9
1bK	2.589	2.700	2.693	1.641			2.860	2.624	1.079	91.3
[c]	2.621	2.741	2.733	1.709			2.894	2.632	1.078	92.9
1cK-1	2.642	2.709	2.693	1.678			3.076	2.414	1.081	118.2
[c]	2.659	2.768	2.752	1.775			3.159	2.434	1.081	123.3
1aK-1	2.727	3.003	2.651	1.832			2.924	2.861	1.080	82.5
[c]	2.770	3.104	2.693	1.931			2.945	2.903	1.079	84.3
1aK-2	2.723	2.661	2.995	1.834			2.914	2.842	1.080	83.0
1bKTHF_1	2.638	2.724	2.719	1.688	3.538	2.657	2.864	2.641	1.079	90.7
[c]	2.657	2.746	2.741	1.728	3.553	2.670	2.885	2.649	1.078	91.5
1aK-1THF_1	2.796	3.021	2.683	1.874	3.557	2.616	2.928	2.874	1.080	82.1
[c]	2.828	3.085	2.711	1.939	3.569	2.626	2.973	2.904	1.079	83.1
1aK-1THF_2	2.806	3.165	2.671	1.951	3.957	2.653	2.957	2.922	1.080	81.2
1aK-2THF_1	2.802	2.695	3.037	1.880	3.791	2.640	2.935	2.886	1.080	81.9

[a] Distance between the M or O and the plane of the three inner N atoms of porphyrin.
[b] The data are from Ref. [7].
[c] In toluene solvent.
[d] Ref. [6].

Finally, the M-NCTPP complexes calculated here are compared with the complexes of the normal tetraphenylporphyrin (TPP) with Li, Na and K [8]. Two types of complexes of TPP have been studied, i.e., $M_2TPP(solvent)_n$ and MTPP (neutral, cation and anion). In the case of $M_2TPP(solvent)_n$ complexes, two inner hydrogen atoms are removed and all three metal cations are out of the plane of the four N atoms [8]. This is in contrast to the insertion of the alkali atom in NCTPP where it causes only one H–N bond to break and the internal C–H bond is retained. In the case of $MTPP^+$, it was found, both experimentally and theoretically, that the attachment of the M^+ cation to normal porphyrin results in the metal lying on top of the porphyrin cavity even for the smallest alkali cation, Li^+ [9]. Note that the two inner hydrogen atoms are still present. Thus the M^+ cations are not effectively sequestered and are in fact exposed and thus accessible for donation [9]. Similarly, M metals are exposed in M-NCTPP and accessible for donation and they can be candidates as intermediates for the preparation of other metal-NCTPP compounds. In the case of Li, neutral π-radicals of monolithium porphyrins LiTPP have been successfully synthesized where the Li atom is in the plane of the porphyrin ring [26]. Calculations have shown that both $LiTPP^+$ and $LiTPP^-$ are also planar [26b]. With inverted porphyrin we found that Li lies close to the plane of the internal N atoms and the distance between Li and the plane is 0.230 Å in the global minimum structure [7], and 0.028 Å in the second minimum. In the LiTPP radical and in $Li_2TPP(OEt_2)_2$ the corresponding values are 0.056 and 1.071 Å, respectively [11], showing that Li complexes of normal and inverted porphyrins present differences with respect to the position of the metal with respect to the porphyrin core.

3.1.3. M-NCTPP-THF

In the presence of THF, pseudo-five coordinate complexes are generated for the lithium complexes of the **1b** porphyrin [6,7]. Similarly, in the case of the sodium and potassium complexes, five coordinate complexes are formed when the oxygen atom of THF is attached to the metal. There is space for only one THF molecule to be complexed with M-NCTPP. Five isomers for Na and six for K have been calculated, labeled as **1*n*MTHF_1** and **1*n*MTHF_2**, (for ***n*** **= a, b, c**) where **1*n*M** are the minima structures of the Na and K complexes of NCTPP; and in the **_1** isomers the ring of THF is parallel to the core, while in the **_2** isomers the THF ring is perpendicular to the core ring, see Figs. 3 and 2S of the ESM. The **_1** structures are slightly lower in energy than the corresponding **_2** structures, in all three functionals and for M = Li, Na and K, see Figs. 3 and 2S of the ESM.

For the complex of Na, the two lowest minima are practically degenerate, i.e., **1aNa-1THF_1** and **1bNaTHF_1**, while in the absence of THF **1bNa** is the global minimum, see Fig. 2. In the case of the complexes of K, the energy difference between the corresponding two minima is larger, i.e., by ∼5 kcal/mol in toluene solvent using the M06-2X functional, and the **1aK-1THF_1** is the global minimum structure, the same as in the absence of THF. The second minimum is the **1aK-1THF_2** structure, which lies ∼2 kcal/mol above the **1aK-1THF_1**. Thus, the presence of THF for the Na complexes of porphyrin decreases the energy difference between the **1bNa** and **1aNa** minima, by ∼2 kcal/mol, while for the K complexes it slightly increases the corresponding difference, see Figs. 2 and 2S of the ESM. Moreover, the presence of the THF in the complexes results in a change of the N-M distances up to 0.3 Å, with the largest increases observed for the **1aNa-1** and **1aK-1** minima, see Table 1. The increase of the N-M distance due to the binging of the M with the THF molecule is predictable because the additional bond attenuates the already existing M-N bonds. Finally, the distance between the M atom and the plane of the three inner N atoms is increased by up to 0.2 Å, for all three M atoms.

3.1.4. Population analyses

The natural population analysis (NPA) and the Mulliken analysis of some of the calculated structures are presented in Table 2, while for all calculated structures the corresponding data are given in Table 1S of the supporting Information. It has been stated that the Mulliken charges can underestimate of the ionic character and present a basis set dependency, while the NPA can overestimate the ionic character of the atoms and it is generally agreed that the use of both population analyses is indicative and helps us to make comparisons for similar structures [27]. Thus, both methods should be used and, via the comparison of the two methods, we may decide on the ionic character of the metals in the complexes. Both analyses predict that the inner N atoms have negative charges which range from −0.6 to −0.7 e^- in all cases. The analyses for the M and the C1 atoms involved in the agostic-like bond predict different charges on the atoms with the NPA predicting more ionic character for the atoms up to 0.3 e^- as it was expected [7]. However, both analyses rank all structures from lowest to highest metal charge, the same way. Moreover, all three functionals predict practically the same charges on the atoms within the same type of

Table 2
Mulliken charges(NPA), $q(e^-)$ of **1**, **1aM**, **1bM, 1cM**, **1aMTHF**, and **1bMTHF** species in the gas phase and at the M06-2X /6-31G(d,p) level of theory; crystallographic data are also included.

Species	q_M	q_{N1}	q_{N2}	q_{N3}	q_O
1bLi[a]	0.34(0.63)	−0.68(−0.60)	−0.67(−0.57)	−0.68(−0.59)	
1cLi-2	0.17(0.57)	−0.64(−0.54)	−0.67(−0.55)	−0.68(−0.56)	
1aLi-1[a]	0.38(0.73)	−0.72(−0.64)	−0.72(−0.61)	−0.69(−0.61)	
1bLiTHF_1[a]	0.28(0.55)	−0.62(−0.60)	−0.63(−0.54)	−0.64(−0.57)	−0.52(−0.59)
1bNa	0.53(0.79)	−0.68(−0.60)	−0.67(−0.58)	−0.68(−0.60)	
1cNa-1	0.56(0.83)	−0.64(−0.55)	−0.63(−0.57)	−0.65(−0.58)	
1cNa-2	0.53(0.80)	−0.64(−0.56)	−0.64(−0.57)	−0.66(−0.58)	
1aNa-1	0.52(0.86)	−0.70(−0.64)	−0.74(−0.64)	−0.66(−0.60)	
1bNaTHF	0.44(0.73)	−0.61(−0.59)	−0.64(−0.56)	−0.65(−0.58)	−0.56(−0.63)
1aNa-1THF_1	0.46(0.82)	−0.69(−0.64)	−0.69(−0.59)	−0.65(−0.60)	−0.56(−0.65)
1aNa-2THF_1	0.44(0.81)	−0.64(−0.62)	−0.66(−0.53)	−0.73(−0.61)	−0.55(−0.64)
1bK	0.71(0.90)	−0.67(−0.61)	−0.66(−0.58)	−0.67(−0.60)	
1cK-1	0.71(0.90)	−0.63(−0.54)	−0.64(−0.56)	−0.65(−0.57)	
1aK-1	0.73(0.92)	−0.72(−0.63)	−0.75(−0.62)	−0.68(−0.59)	
1bKTHF	0.64(0.83)	−0.62(−0.59)	−0.65(−0.56)	−0.66(−0.58)	−0.57(−0.63)
1aK-1THF_1	0.66(0.86)	−0.67(−0.61)	−0.74(−0.61)	−0.66(−0.57)	−0.58(−0.64)
1aK-2THF_1	0.65(0.86)	−0.69(−0.61)	−0.65(−0.57)	−0.75(−0.61)	−0.56(−0.63)

[a] The data are from Ref. [7].

Table 3
Reaction energies, ΔE^a (kcal/mol), enthalpies $\Delta H^{a,b}$(kcal/mol) and Gibbs free energies $\Delta G^{a,b}$(kcal/mol) for the fragmentation of the M-NCTPP molecule, M = Li, Na and K in the gas phase (in toluene solvent) at the M06-2X/6-31G(d,p) level of theory.[c].

	M-NCTPP → M + NCTPP		M-NCTPP → M^+ + $NCTPP^-$	
	1bLi	1aLi-1	1bLi	1aLi-1
ΔE	129.7(123.2)	106.1(103.3)	201.5(108.4)	166.2(78.0)
ΔH	127.8(121.5)	104.4(101.6)		164.1(80.3)
ΔG	118.9(113.0)	94.0(91.5)	192.0(100.2)	155.1(67.9)
	1bNa	1aNa-1	1bNa	1aNa-1
ΔE	101.1(99.1)	85.4(87.1)	167.3(88.6)	140.0(66.2)
ΔH	99.8(98.0)	84.2(85.7)	165.8(91.9)	138.4(68.7)
ΔG	90.3(88.6)	73.9(75.7)	157.8(80.2)	129.5(56.4)
	1bK	1aK-1	1bK	1aK-1
ΔE	93.1(92.9)	84.0(86.8)	138.5(73.4)	117.8(56.8)
ΔH	91.9(91.9)	83.1(85.9)	137.2(76.3)	116.6(59.4)
ΔG	82.0(82.1)	73.2(76.3)	128.7(84.6)	108.0(48.0)

[a] BSSE corrected values.
[b] At 1 atm and 298.15 K.
[c] The ΔE, ΔH, and ΔG values have been calculated with respect to the corresponding isomer of the **1a** or **1b**.

Table 4
Reaction energies, ΔE^a (kcal/mol), enthalpies $\Delta H^{a,b}$(kcal/mol) and Gibbs free energies $\Delta G^{a,b}$(kcal/mol) for the formation of the **1*n*M** and **1*n*MTHF** species, where *n* = a and b and M = Li, Na, and K, for the NCTPP + $MN(Si(Me)_3)_2$ → M-NCTPP + $HN(Si(Me)_3)_2$ or NCTPP + $MN(Si(Me)_3)_2$ + THF → M-NCTPP-THF + $HN(Si(Me)_3)_2$ reactions in the gas phase (in toluene solvent) at the M06-2X/6-31G(d,p) level of theory.

	1bM[c]	1bMTHF_1[c]	1aM-1[c]	1aM-1THF_1[c]
M = Li[d]				
ΔE	−47.7(−37.3)	−67.6(−55.4)	−37.2(−28.5)	
ΔH	−48.1(−37.6)	−65.2(−54.1)	−37.4(−28.7)	
ΔG	−47.6(−37.1)	−53.6(−42.5)	−36.2(−27.5)	
M = Na				
ΔE	−36.6(−28.0)	−56.0(−44.7)	−33.6(−27.0)	−55.3(−44.9)
ΔH	−36.1(−28.0)	−52.7(−41.7)	−33.2(−26.8)	−52.6(−42.6)
ΔG	−35.0(−26.8)	−40.2(−29.2)	−32.1(−26.0)	−42.0(−32.0)
M = K				
ΔE	−27.7(−22.2)	−45.3(−37.1)	−31.4(−27.0)	−49.9(−42.6)
ΔH	−27.8(−22.0)	−43.3(−34.7)	−31.7(−27.1)	−47.7(−40.0)
ΔG	−25.0(−19.7)	−30.4(−22.4)	−29.8(−26.1)	−35.1(−28.0)

[a] BSSE corrected values.
[b] At 1 atm and 298.15 K.
[c] The ΔE, ΔH, and ΔG values have been calculated with respect to the most stable **1a** isomer of the NCTPP.
[d] Ref. [7].

analysis. Roughly, the Na and K metal atoms have a charge of about 0.7 and 0.8 e^-, respectively, cf. 0.5 e^- calculated for Li [7]. Note, that the occupancy of the axial position in the complex by THF results in a small reduction of the positive charge of the metals for both analyses because THF is connected to the M metal via its empty p_z orbital and charge is transferred to M from the O atom of THF. The Na and K metals have the same ionic charge within the same analyses for all the **1aM, abM** and **1cM** complexes, while in the case of the **1cLi-2** complex Li has less ionic character than in the **1bLi** and **1aLi** complexes. Note that the **1cLi-2** complex is a planar complex. Overall, on the contrary to Li complexes [7], the Na and K species are have a stronger ionic character than Li and the Na and K complexes adopt a more typical tetrahedral coordination of Na^+ and K^+ [8].

3.2. Energetics

The strength of the M–N bond was calculated for the three M metals and their different isomers see Tables 3 and 2S of the ESM. The strength of the M–N bond decreases in going from the Li to the K complexes, both with respect to the homolytic and the heterolytic cleavage of the M–N bond. The presence of toluene reduces the strength of the M–N bond slightly in the homolytic cleavage, i.e., by about 6 kcal/mol for Li, ~2 kcal/mol for Na and ~0 kcal/mol for K. On the contrary, in the heterolytic cleavage the bond strength is reduced in toluene to about half of the value in the gas phase, see Table 3. Thus, concerning the potential use of the M-NCTPP as a synthetic reagent for the preparation of other metal-NCTPP, K-NCTPP is the best reagent among the three calculated here. The same stands for the corresponding normal porphyrins [11]. Finally, the heterolytic cleavage of the bond strength in toluene is the least expensive route for severing the M–N bond with reaction enthalpies (at 1 atm and 298.15 K) of 80.3, 68.7, and 59.4 kcal/mol for the Li-NCTPP, Na-NCTPP, and K-NCTPP, respectively.

The insertion of sodium and potassium into **1** has been calculated for the reaction:

$$\mathrm{NCTPP} + \mathrm{MN(Si(Me)_3)_2} \rightarrow \mathrm{M\text{-}NCTPP} + \mathrm{HN(Si(Me)_3)_2} \quad (1)$$

The M06-2X reaction enthalpies of reaction (1) at 1 atm and 298.15 K are -48.1(-37.6) kcal/mol for the production of the Li-NCTPP (**1bLi**) [7], −36.1(−28.0) for the Na-NCTPP (**1bNa**), and −31.7(−27.1) for the K-NCTPP (**1aK-1**), with respect to the lowest energy **1a** tautomer in the gas phase (in toluene solvent), see Table 4. In the presence of THF, the reaction enthalpies for the formation of the lowest energy isomers, are −65.2(−54.1), −52.7(−41.7) and −47.7(−40.0) kcal/mol, respectively, the values decreasing with the size of the metal, i.e., the Li-NCTPP complex is the most stable among the three M-NCTPP complexes.

Reaction (1) is probably a multi-step reaction. The M–N bond of the $MN(Si(Me)_3)_2$ reagent can be homolytically or heterolytically broken in the first step, followed by the substitution of the H atoms or cations attached to the internal N atoms of NCTPP with the M atom or cations and finally the formation of the $HN(Si(Me)_3)_2$ molecule, cf., reactions (2)–(4) for the homolytic procedure and reactions (5)–(7) for the heterolytic procedure.

$$\mathrm{MN(Si(Me)_3)_2} \rightarrow \mathrm{M^{\cdot}} + \mathrm{{\cdot}N(Si(Me)_3)_2} \quad (2)$$

$$\mathrm{NCTPP} + \mathrm{M^{\cdot}} \rightarrow \mathrm{M\text{-}NCTPP} + \mathrm{H^{\cdot}} \quad (3)$$

$$\mathrm{H^{\cdot}} + \mathrm{{\cdot}N(Si(Me)_3)_2} \rightarrow \mathrm{HN(Si(Me)_3)_2} \quad (4)$$

$$\mathrm{MN(Si(Me)_3)_2} \rightarrow \mathrm{M^+} + \mathrm{{}^-N(Si(Me)_3)_2} \quad (5)$$

$$\mathrm{NCTPP} + \mathrm{M^+} \rightarrow \mathrm{M\text{-}NCTPP} + \mathrm{H^+} \quad (6)$$

$$\mathrm{H^+} + \mathrm{{}^-N(Si(Me)_3)_2} \rightarrow \mathrm{HN(Si(Me)_3)_2} \quad (7)$$

The reaction energies, the enthalpies and the Gibbs free energies of the above reactions are given in Table 4 and Tables 3S–4S of the ESM. The relative enthalpies in toluene solvent of these two possible routes are depicted in Figs. 5 and 6 for M = Na and K, respectively, while the enthalpies for the insertion of Li, Na and K via the reaction both in the gas phase and in toluene solvent are depicted in Figs. 3S–5S of the ESM. These three figures have the same patern, showing that the reaction enthalpies of formation for the three metals have the same trends with respect to where the reaction occurs, i.e., in the gas phase or in toluene solvent, and how it occurs, i.e., via heterolytic or homolytic route. Moreover, it seems that even though the toluene solvent stabilizes the heterolytic route substantially, the metal insertion is more likely to occur via the homolytic route rather than the heterolytic route for all three metals. The only difference between the three metals

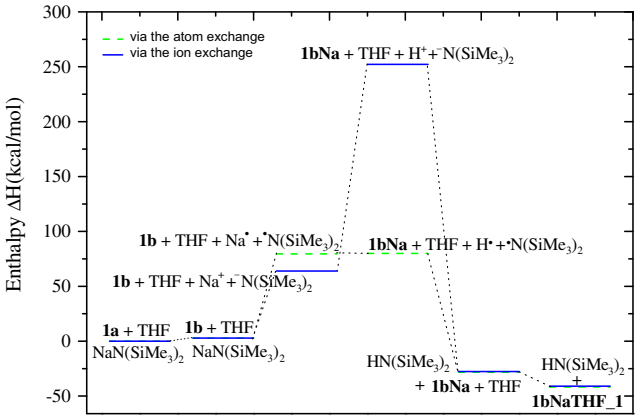

Fig. 5. Enthalpies for the insertion of sodium via the reaction **1b** + $NaN(Si(Me)_3)_2$ + -THF → **1bNaTHF_1** + $HN(Si(Me)_3)_2$ in toluene solvent via the atom exchange or the ion exchange at the M06-2X/6-31G(d,p) level of theory, at 1 Atm and 298.15 K.

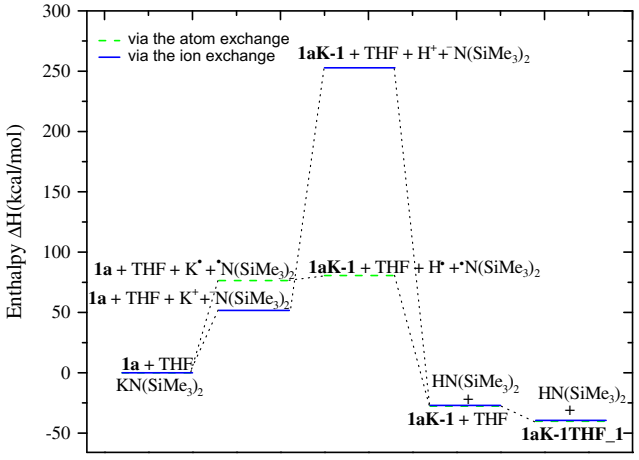

Fig. 6. Enthalpies for the insertion of potassium via the reaction **1a** + $KN(Si(Me)_3)_2$ + THF → **1aK-1THF_1** + $HN(Si(Me)_3)_2$ in toluene solvent via the atom exchange or the ion exchange at the M06-2X/6-31G(d,p) level of theory, at 1 atm and 298.15 K.

is that reaction (3) is exothermic for Li (ΔH = −20.3 kcal/mol in toluene solvent) while it is endothermic for Na (3.2) and K (4.2), see Table 3S and Figs. 3S–5S of the ESM.

The presence of the THF provides additional stabilization to the M-NCTPP complexes because of the extra bond O–M that is formed. The M06-2X calculated interaction energies of the **1*n*M** with THF are similar for all three metals and range from −17.2 to −21.3 and from −14.5 to −17.6 kcal/mol in the gas phase and in toluene solvent, respectively, see Table 5. The largest interaction energies are predicted for M = Na. Note that, the interactions between THF and **1a**(**1b**) are −15.4(−10.5) kcal/mol, in toluene [7], smaller than the corresponding values of the THF and **1*n*M**.

3.3. Absorption spectra

The Gouterman's 4 electron-4 orbital model [28], which explains the absorption spectra of porphyrins, assumes that the absorption bands in porphyrin systems arise from transitions between two HOMO (H, H–1) and two LUMO (L, L+1) orbitals. The identities of the metal center and the substituents on the ring affect the relative energies of these transitions. Transitions between these orbitals give rise to Q-bands and the Soret (or B) band. The Q bands are responsible for the red to purple color, are present in the visible region between 500 and 700 nm of the free base porphyrin absorption spectra. The Soret band is a very sharp and intense band which appears around 400 nm in the near UV region. There are also additional bands (N, L, M bands) in the UV, but these are usually quite weak. The Soret band positions are sensitive to substituent groups. [29] This model is also applicable to N-confused free and metal porphyrins [7,10]. Since the Q and Soret bands are the most important ones in the study of the absorption spectra of porphyrins, attention will be given mainly to these bands.

In this section, we study the absorption spectra of the M-NCTPP complexes using the TD-B3LYP, TD-M06-2X, and TD-PBE0 functionals. The TD-B3LYP functional predicts Q and Soret peaks for the Li-NCTPP and its externally N-methylated complex [7] in very good agreement with the experimental values [6], while for TD-CAM-B3LYP and TD-M06-2X these peaks are similar and are shifted to larger energies [7]. The TD-PBE0 functional is a reliable functional for the study of excited electronic states of organic molecules [18,19] and for free normal porphyrin as it has been seen from comparison of TD-PBE0 spectra with the experimental data [19]. Finally, the TD-M06-2X functional is used here to see if for the Na-NCTPP and K-NCTPP complexes it presents absorption spectra similar with TD-B3LYP spectra.

All the calculated absorption spectra of the studied minima in the gas phase and in toluene solvent with all three functionals are presented in Figs. 6S–11S of the ESM, while the TD-PBE0 calculated absorption spectra are depicted in Fig. 7. These figures have been visualized by GaussView5 [25] and they depict the molar absorptivity, ε versus wavelength (labeled by GaussView5 as excitation energy, in nm). The molar absorptivity is directly related to the dipole transition moments. The peak half-widths at half height are 0.05 eV. Excitation energies (ΔE), major peaks (λ), oscillator strengths (f-value), main excitations and their coefficient contributing to the excited state of calculated structures for the lowest-energy Q and Soret bands, calculated via TD-DFT, are given in Table 6 and Tables 5S and 6S of the ESM.

The experimental absorption spectrum of the Li-NCTPP complex [6] is used as a guide for evaluation of the PBE0 applicability. We find here that the TD-PBE0 peak shifts range from 0.01 to 0.23 eV. Specifically, the PBE0 λ values of the lowest-energy Q and major Soret peaks determined at 742 and 431 cm^{-1}, are in good agreement with the experimental values of 739 and 468 cm^{-1}, see Table 6. Note that the TD-B3LYP peak shifts range from 0.06 to 0.16 eV, while TD-M06-2X presents for the major Soret peak a blue shift of 0.4 eV, Table 6. We observe that the TD-PBE0 values are between the TD-B3LYP and the TD-M06-2X values and

Table 5
BSSE corrected interaction energies in kcal/mol of the **1aM** and **1bM** species, where M = Li, Na, and K with the THF molecule in the gas phase (in toluene solvent) at the B3LYP, PBE0, and M06-2X/ 6-31G(d,p) levels of theory.

	1bLiTHF_1[a]	1aNa-1THF_1	1bNaTHF_1	1aK-1THF_1	1bKTHF_1
B3LYP	−7.5(−5.9)	−14.6(−11.2)	−11.3(−9.1)	−11.5(−8.7)	−9.6(−7.3)
PBE0	−10.2(−8.4)	−17.2(−12.5)	−12.8(−10.2)	−12.9(−10.0)	−11.6(−9.1)
M06-2X	−19.3(−17.6)	−21.3(−17.6)	−19.1(−16.4)	−18.1(−14.9)	−17.2(−14.5)

[a] Ref. [7].

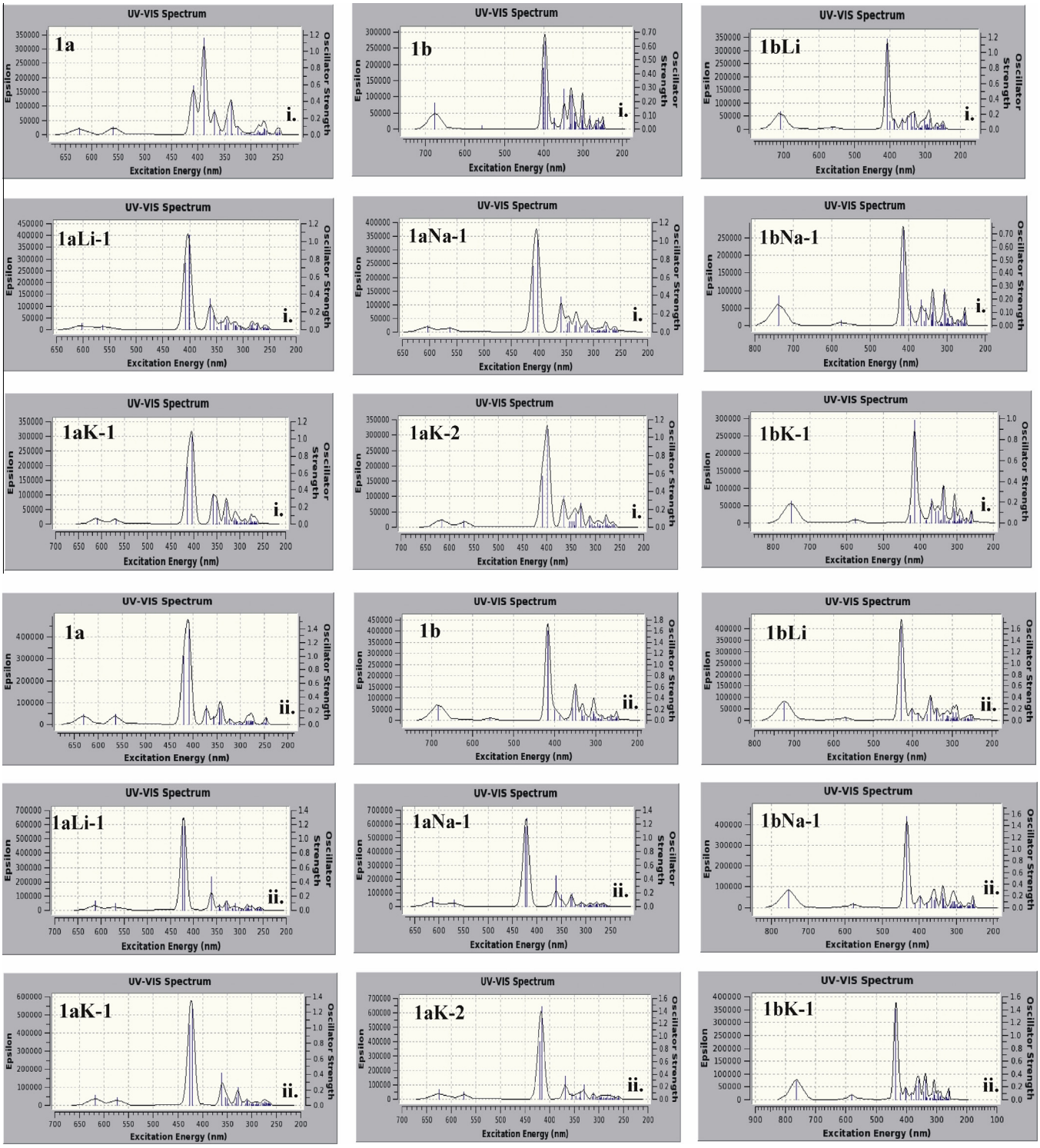

Fig. 7. Absorption spectrum (molar absorptivity, ε versus excitation energy) of **1a**, **1b**, **1bM**, **1aM** species, where M = Li, Na, and K, (**i.**) in the gas phase and (**ii.**) in toluene solvent calculated at the TD-PBE0/6-31G(d,p) level of theory. The absorption spectra of all calculated species in the gas phase and in toluene at the TD-B3LYP, TD-PBE, and TD-M06-2X/6-31G(d,p) levels of theory are given in the supporting information.

are more similar to the TD-B3LYP values than to the TD-M06-2X ones, see Tables 6 and 5S–6S of the ESM. As a conclusion both B3LYP and PBE0 functionals are considered as a good choice for the calculation of the spectra in the present work, while the M06-2X peaks are shifted to larger energies by 0.1–0.3 eV with respect to B3LYP peaks. As mentioned above the Q and Soret bands result from transitions between H, H-1 and L, L+1 orbitals, see Fig. 8. The fact that the excited states are well described with the B3LYP or PBE0 functionals stems from the fact that the electronic excitations are not of the charge-transfer type. Note that if they were of the charge-transfer type the CAM-B3LYP should be used.

However, all three functionals predict the same general shape of the vis–UV spectra for the same minimum; see Figs. 6S–11S of the ESM and for the case of Li-NCTPP these spectra are in

Table 6
Excitation energies, ΔE_e(eV), absorption selected peaks (lowest-energy Q and major soret peaks), λ(nm), oscillator strengths, f, main excitations and their coefficient contributing to the excited state of the **1a**, **1b**, **1aM**, **1bM**, **1aMTHF**, and **1bMTHF** species, where M = Li, Na, and K in toluene solvent at the B3LYP, PBE0 and M06-2X /6-31G(d,p) levels of theory.

	B3LYP			PBE0			M06-2X			Expt[b]
	ΔE_e	λ	f	ΔE_e	λ	f	ΔE_e	λ	f	λ
1a[a]	1.93	644	0.13	1.97	631	0.15	1.99	624	0.11	
	2.97	417	1.45	3.03	409	1.49	3.13	396	1.59	
1b[a]	1.76	703	0.24	1.82	683	0.26	2.03	609	0.26	
	2.90	427	1.46	2.97	417	1.61	3.15	393	1.75	
1aLi[a]	1.98	625	0.12	2.02	612	0.13	2.07	598	0.09	
	2.89	429	1.25	2.93	423	1.29	3.03	409	1.59	
1bLi[a]	1.67	744	0.29	1.71	725	0.32	1.83	679	0.34	
	2.83	438	1.56	2.89	429	1.64	3.04	404	1.75	
1bLiTHF_1[a]	1.62	765	0.27	1.67	742	0.29	1.79	692	0.31	739
	2.81	442	1.43	2.87	431	1.51	3.05	407	1.59	468
1bLiTHF_2[a]	1.62	767	0.27	1.67	742	0.29	1.80	690	0.31	
	2.81	442	1.43	2.88	431	1.51	3.05	406	1.62	
1aNa-1	1.97	631	0.14	2.04	612	0.13	2.11	589	0.08	
	2.87	431	1.26	2.95	420	1.28	3.04	407	1.58	
1bNa	1.60	775	0.29	1.65	753	0.31	1.76	705	0.34	
	2.79	444	1.42	2.86	434	1.56	3.05	407	1.71	
1aNa-1THF_1	1.95	634	0.13	2.02	615	0.12	2.07	599	0.08	
	2.87	432	1.21	2.95	420	1.26	3.03	410	1.45	
1aNa-2THF_1	1.94	640	0.14	1.98	626	0.15	2.05	603	0.11	
	2.90	428	1.34	2.97	418	1.32	3.05	406	1.58	
1bNaTHF_1	1.60	777	0.27	1.64	754	0.29	1.75	706	0.32	
	2.79	445	1.33	2.86	433	1.50	3.04	407	1.65	
1aK-1	1.94	639	0.14	2.01	618	0.13	2.09	593	0.08	
	2.86	433	1.24	2.95	421	1.31	3.04	408	1.57	
1aK-2	1.92	645	0.15	1.99	624	0.15	2.05	605	0.11	
	2.89	429	1.37	2.98	416	1.48	3.06	405	1.63	
1bK	1.58	787	0.27	1.62	763	0.29	1.74	712	0.32	
	2.77	448	0.72	2.85	434	1.41	3.05	407	1.64	
1aK-1THF_1	1.93	642	0.14	2.00	620	0.13	2.07	600	0.09	
	2.86	434	1.22	2.94	421	1.30	3.02	410	1.59	
1aK-2THF_1	1.91	649	0.15	1.95	636	0.16	2.05	606	0.11	
	2.89	430	1.33	2.96	420	1.28	3.06	405	1.57	
1bKTHF_1	1.57	790	0.26	1.62	766	0.28	1.73	718	0.31	
	2.81	442	0.82	2.85	435	1.36	3.03	409	1.63	

[a] The B3LYP and M06-2X data are from Ref. [7].
[b] Ref. [6].

agreement with the full shape of the experimental spectrum which has been derived for wavelengths from 350 to 775 nm. All complexes which include the same isomer, i.e., **a**, **b**, or **c**, have the same general shape of the vis–UV spectra, irrespectively of the M metal or the existence of the THF. There are differences between the spectra of the minima in the gas phase and in toluene solvent mainly in the relative position of the two Soret peaks and in the spectra under the 400 nm, see Fig. 7 and compare Figs. 6S–8S to Figs. 9S–11S. The presence of the THF almost does not change the Q and Soret bands, see Fig. 6S–11S. On the contrary, in free **1a** NCTTP the presence of THF affect a little the position of the Q and Soret band, for example in toluene solvent the TD-B3LYP peaks are at 644 and 417 cm^{-1}, in the presence of the one THF moved to 689 and 425 [7], while the experimental values are 710 and 443 cm^{-1} [6].

The M06-2X electron density plots of the frontier orbitals, i.e., H−1, H (HOMO), L (LUMO), and L+1, of the **1**, **1aM**, **1bM**, **1cM**, **1aMTHF**, and **1bMTHF** species are depicted in Fig. 8 and in Figs. 9S-11S of the ESM. The different isomers **a**, **b**, or **c** have almost the same H−1, H, L, and L+1 orbitals, irrespective of the substitution of H by M. Additionally, the presence of the THF molecule does not change the general shape of these orbitals. The only difference with respect to the M atom or to the presence of THF is small energy differences of the orbitals, see Table 7S of the ESM. Moreover, for all different **a** and **b** isomers the energy difference between H and H−1 orbitals is larger than the energy difference between L and L+1 orbitals, a typical case for the low-symmetry porphyrin compounds [30]. On the other hand, for all different **c** isomers the opposite occurs, irrespective of the H or the M atom or to the presence of the THF molecule. In addition, it seems from Fig. 8 and in Figs. 9S–11S of the ESM, that the inverted nitrogen atom contributes to the porphyrin H-1 and L orbitals and not in H and L+1 orbitals for all different **a** and **b** isomers; while for all different **c** isomers it contributes to the four frontier orbitals. Finally, the metal does not contribute to the H−1, H, L and L+1 orbitals.

As mentioned above, excitations among the H−1, H, L, and L+1 orbitals result in the transitions of the Q and Soret (B) bands [7]. The lowest energy Q peak, i.e., first excited state, in the **b** isomers is a H → L transition and in the **a** and **c** isomers is dominated by this transition, irrespective of the H or the M atom or the presence of the THF molecule. The major peak of the Soret band corresponds to excitation from the H−1 to the L orbital (having the largest coefficient) and from the H to the L+1 orbital, for almost all minima, see Table 5S of the ESM. Note that all three functionals yield the same main excitations and coefficient contributing to the excited state. In the **a** isomers the lowest energy Q peak is blue shifted as the hydrogen atom is replaced by the M metal. On the contrary, in the **b** isomers the lowest energy Q peak is red shifted as the H is replaced by the M metal. In both **a** and **b** isomers, as the M's size is increased, the lowest energy Q peak is red shifted. In the **c** isomers the lowest energy Q peak is red shifted as the hydrogen atom is replaced by the M metal, and all three metals have similar values for the Q peak. These shifts depict the reduction (red shifts) or the increase (blue shifts) in the H–L gap, see Table 5. Finally, the major peak of the Soret band is red shifted as the M size is increased. Note that these trends are observed with TD-B3LYP and TD-PBE0

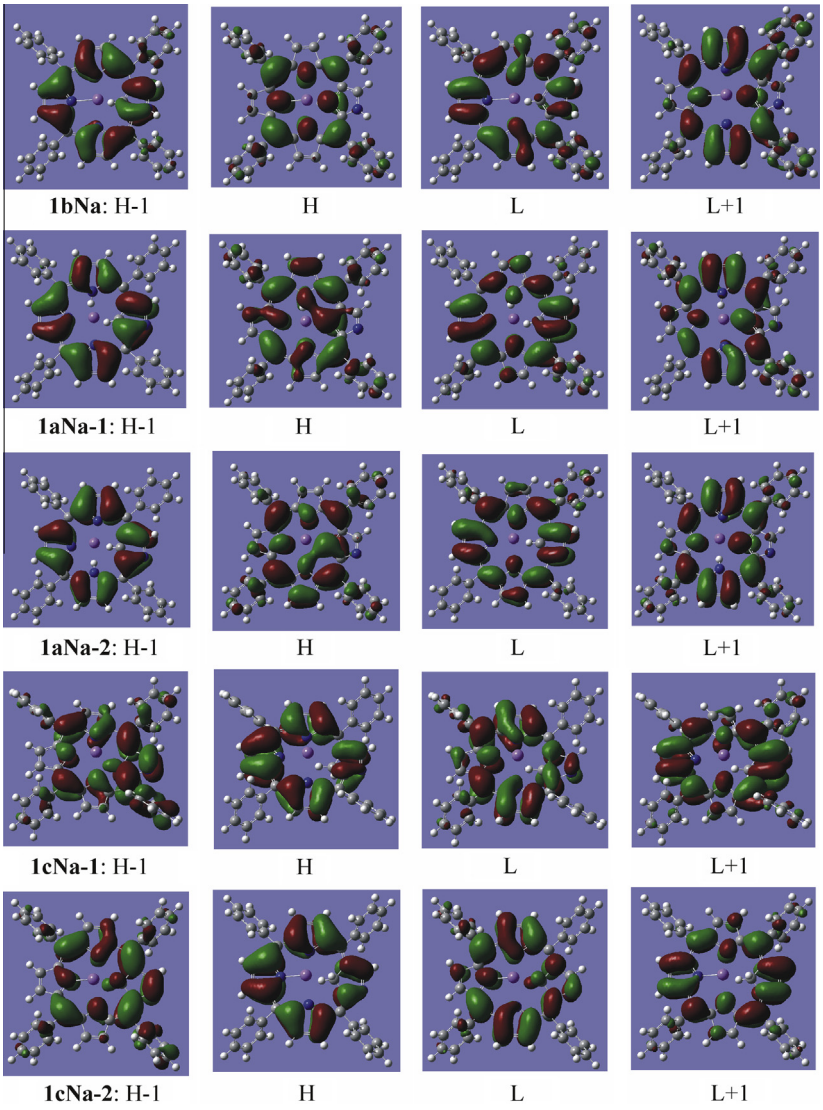

Fig. 8. Plots of the M06-2X frontier orbitals for the **1aNa**, **1bNa**, and **1cNa** species.

functionals. The TD-M06-2X do not follow these trends for all minimum structures, however, all peak shifts are very small.

Additional N, L, M bands observed in the UV spectra are located at ~350, ~330, ~280 nm using the TD-B3LYP and TD-PBE0 functionals, see Figs. 7 and 6S–11S of the ESM. The corresponding TD-M06-2X peaks are blue shifted by about 20 nm with respect to TD-B3LYP and TD-PBE0 values.

Overall, even though the metal does not contribute to the H−1, H, L and L+1 orbitals, it causes a small effect in the energy of the orbitals resulting in red shifts in the lowest energy Q peaks for the global minima of the structures as the metal size increases from Li to K and small shifts in the Soret band.

4. Conclusions

The present work is the first study on sodium and potassium complexes of N-confused tetraphenylporphyrins (NCTPP) employing the theoretical methods DFT and TD-DFT and the B3LYP, PBE0 and M06-2X functionals in conjunction with the 6-31G(d,p) basis set. Additional calculations on lithium complexes were also carried out. The purpose of the present study is to determine the stability, binding, absorption spectra and reaction energy of the formation as well as the differences between the complexes of NCTPP with lithium, sodium and potassium. A summary of our main results follows.

The global minimum and the relative ordering of the stable minima of the M-NCTPP change for the different M, where M = Li, Na and K. The global minimum energy structures of sodium and potassium complexes of NCTPP result from different tautomers of the porphyrin, **1b** and **1a**. The THF and the toluene solvent affect the energy ordering of different low-lying minimum energy structures.

All functionals predict similar geometries. The distance between the M atom and the plane of the three inner N atoms ranges from 0.0 to 0.7 Å for the **1*n*Li** minima, while the corresponding distances increase for the **1*n*Na** and **1*n*K** minima, which range from 0.9 to 1.2 and from 1.6 to 1.8 Å, respectively.

The insertion of Li, Na and K into N-confused porphyrin, in the presence of THF is exothermic with a reaction energy calculated to be −68(−55), −56(−45) and −50(−43) kcal/mol in the gas phase (in toluene solvent), and using the corresponding metal bis-(trimethylsilyl)amide reagent, respectively. It appears that even though the toluene solvent stabilizes the heterolytic route substantially, the metal insertion is more likely to occur via the homolytic route rather than the heterolytic route for all three metals.

The strength of the M–N bond decreases in going from the Li to the K complexes, both with respect to the homolytic and the heterolytic cleavage of the M–N bond. The heterolytic cleavage of the bond strength in toluene is the most likely route for the severing of the M–N bond with reaction enthalpies (at 1 atm and 298.15 K) of 80.3, 68.7, and 59.4 kcal/mol for the Li-NCTPP, Na-NCTPP, and K-NCTPP, respectively.

All three functionals predict the same general shape of the vis–UV spectra for the same minimum. The TD-PBE0 and the TD-B3LYP methods are considered as good choices for the calculation of the absorption spectra. The absorption spectra are similar for the different metals and small red shifts are observed for the same minimum structure as the metal changes from Li to K for the Q and Soret bands. Peak positions in toluene solvent are red shifted up to 22 nm with respect to the corresponding spectra in the gas phase.

The different results obtained for the three metals derive from the fact that N-M distance is increased from Li to K. While Li is small enough to fit in the porphyrin core, Na and K form more elongated N-M bonds, hence they do not fit in the core and are located above it. Additionally, the M-N bonds are energetically weaker than the Li–N bond. The fact that Na and K are above the porphyrin core causes the metal atom to be effectively sequestered and be in fact exposed and thus accessible for donation.

The present work provides information for the potential use of alkali metal NCP as synthetic reagents like the alkali metal normal porphyrins do. It seems that K-NCTPP is the best reagent among the three calculated here.

Appendix A. Supplementary material

Supplementary data associated with this article can be found, in the online version, at http://dx.doi.org/10.1016/j.comptc.2013.07.014.

References

[1] (a) H. Furuta, T. Asano, T. Ogawa, "N-confused porphyrin": a new isomer of tetraphenylporphyrin, J. Am. Chem. Soc. 116 (1994) 767–768;
(b) P.J. Chmielewski, L. Latos-Grażyński, K. Rachlewicz, T. Glowiak, Tetra-p-tolylporphyrin with an inverted pyrrole ring: a novel isomer of porphyrin, Angew. Chem. Int. Ed. Engl. 33 (1994) 779–781.

[2] (a) H. Furuta, H. Maeda, A. Osuka, Confusion, inversion, and creation—a new spring from porphyrin chemistry, Chem. Commun. (2002) 1795–1804;
(b) S.K. Pushpan, T. Chandrashekar, Aromatic core-modified expanded porphyrinoids with *meso*-aryl substituents, Pure Appl. Chem. 74 (2002) 2045–2055;
(c) J.D. Harvey, C.J. Ziegler, Developments in the metal chemistry of N-confused porphyrin, Coord. Chem. Rev. 247 (2003) 1–19;
(d) A. Ghosh, A perspective of one-pot pyrrole–aldehyde condensations as versatile self-assembly processes, Angew. Chem. Int. Ed. 43 (2004) 1918–1933;
(e) A. Srinivasan, H. Furuta, Confusion approach to porphyrinoid chemistry, Acc. Chem. Res. 38 (2005) 10–20;
(f) P.J. Chmielewski, L. Latos-Grażyński, Core modified porphyrin-a macrocyclic platform for organometallic chemistry, Coord. Chem. Rev. 249 (2005) 2510–2533;
(g) A. Çetin, W.S. Durfee, C.J. Ziegler, Low-coordinate transition-metal complexes of a carbon-substituted hemiporphyrazine, Inorg. Chem. 46 (2007) 6239–6241;
(h) H.-W. Jiang, Q.-Y. Chen, J.-C. Xiao, Y.-C. Gu, Synthesis and reactions of the first fluoroalkylated Ni(II) N-confused porphyrins, Chem. Commun. (2008) 5435–5437;
(i) P.J. Chmielewski, Synthesis and characterization of transition metal complexes of dimeric N-confused porphyrin linked by an o-xylene fragment, Inorg. Chem. 48 (2009) 432–445.

[3] (a) C.-H. Hung, W.-C. Chen, G.-H. Lee, S.-L. Peng, Dimeric iron n-confused porphyrin complexes, Chem. Commun. (2002) 1516–1517;
(b) I. Schmidt, P.J. Chmielewski, Z. Ciunik, Alkylation of the inverted porphyrin nickel(II) complex by dihalogenalkanes: formation of monomeric and dimeric derivatives, J. Org. Chem. 67 (2002) 8917–8927;
(c) H. Maeda, H. Furuta, N-confused porphyrins as new scaffolds for supramolecular architecture, J. Porphyr. Phthalocya. 8 (2004) 67–75;
(d) H. Furuta, T. Morimoto, A. Osuka, Structures and ligand exchange of N-confused porphyrin dimer complexes with group 12 metals, Inorg. Chem. 43 (2004) 1618–1624;
(e) H. Maeda, H. Furuta, A dozen years of N-confusion: from synthesis to supramolecular chemistry, Pure Appl. Chem. 78 (2006) 29–44;
(f) M. Toganoh, N. Harada, T. Morimoto, H. Furuta, Experimental and theoretical studies on oligomer formation of N-confused porphyrin-zinc(II) complexes, Chem. Eur. J. 13 (2007) 2257–2265 (and reference therein).

[4] (a) H. Maeda, T. Morimoto, A. Osuka, H. Furuta, Halide anion binding by singly and doubly N-confused porphyrin, Chem. Asian J. 1 (2006) 832–844;
(b) V. Yeguas, G.I. Cárdenas-Jirón, M.L. Menéndez, R. López, A computational study on the stability–aromaticity correlation of triply N-confused porphyrins: CMMSE-09, J. Math. Chem. 48 (2010) 137–144 (and reference therein).

[5] (a) Z. Xiao, B.O. Patrick, D. Dolphin, Inner C-cyanide addition and nucleophilic addition to Ni(II) N-confused porphyrins, Chem. Commun. (2003) 1062–1063;
(b) K. Rachlewicz, S.L. Wang, C.-H. Peng, C.-H. Hung, L. Latos-Grażyński, Remarkable paramagnetically shifted ^{1}H and ^{2}H NMR spectra of iron(II) complexes of 2-aza-21-carbaporphyrin: an evidence for agostic interaction, Inorg. Chem. 42 (2003) 7348–7350;
(c) K. Rachlewicz, S.-L. Wang, J.-L. Ko, C.-H. Hung, L. Latos-Grażyński, Oxidation and oxygenation of iron complexes of 2-Aza-21-carbaporphyrin, J. Am. Chem. Soc. 126 (2004) 4420–4431;
(d) X. Zhu, W.-K. Wong, W.-K. Lo, W.-Y. Wong, Synthesis and crystal structure of the first lanthanide complex of N-confused porphyrin with an η^2 agostic C–H interaction, Chem. Commun. (2005) 1022–1024;
(e) C.-H. Hung, C.-H. Chang, W.-M. Ching, C.-H. Chuang, Molecular assembling using axial phenolate on an iron N-confused porphyrin complex, Chem. Commun. (2006) 1866–1868;
(f) F. D'Souza, P.M. Smith, L. Rogers, M.E. Zandler, D.M. Shafiqul Islam, Y. Araki, O. Ito, Formation, spectral, electrochemical, and photochemical behavior of zinc N-confused porphyrin coordinated to imidazole functionalized fullerene dyads, Inorg. Chem. 45 (2006) 5057–5065;
(g) T. Ishizuka, H. Yamasaki, A. Osuka, H. Furuta, Syntheses of aryl- and arylethynyl-substituted N-confused porphyrins, Tetrahedron 63 (2007) 5137–5147;
(h) S.-W. Hung, F.-A. Yang, J.-H. Chen, S.-S. Wang, J.-Y. Tung, Magnetic susceptibility and ground-state zero-field splitting in high-spin mononuclear manganese(III) of inverted n-methylated porphyrin complexes: Mn(2-NCH_3NCTPP)Br, Inorg. Chem. 47 (2008) 7202–7206;
(i) S. Sripothongnak, C.J. Ziegler, M.R. Dahlby, V.N. Nemykin, Controllable and reversible inversion of the electronic structure in nickel N-confused porphyrin: a case when MCD matters, Inorg. Chem. 50 (2011) 6902–6909.

[6] S. Sripothongnak, C.J. Ziegler, Lithium complexes of N-confused porphyrin, Inorg. Chem. 49 (2010) 5789–5791.

[7] D. Tzeli, I.D. Petsalakis, G. Theodorakopoulos, Computational insight into the electronic structure and absorption spectra of lithium complexes of N-confused tetraphenylporphyrin, J. Phys. Chem. A 115 (2011) 11749–11760.

[8] J. Arnold, D.Y. Dawson, C.C. Hoffman, Synthesis and characterization of lithium, sodium, and potassium porphyrin complexes. X-ray crystal structures of $Li_2(C_6H_{12}O_2)_2$TMPP, $Na_2(THF)_4$OEP, and K_2(pyridine)$_4$OEP, J. Am. Chem. Soc. 115 (1993) 2707–2713.

[9] J.J.A. van Kampen, T.M. Luider, P.J.A. Ruttink, P.C. Burgers, Metal ion attachment to the matrix meso-tetrakis(pentafluorophenyl)porphyrin, related matrices and analytes: an experimental and theoretical study, J. Mass Spectrom. 44 (2009) 1556–1564.

[10] S. Vyas, C.M. Hadad, D.A. Modarelli, A computational study of the ground and excited state structure and absorption spectra of free-base N-confused porphine and free-base N-confused tetraphenylporphyrin, J. Phys. Chem A 112 (2008) 6533–6549.

[11] J. Arnold, in: K.M. Kadish, K.M. Smith, R. Guilard (Eds.), The Porphyrin Handbook: Inorganic, Organometallic and Coordination Chemistry, vol. 3, Academic Press, San Diego, 2000, pp. 115–127.

[12] (a) D. Becke, A new mixing of Hartree-Fock and local density-functional theories, J. Chem. Phys. 98 (1993) 1372–1377;
(b) C. Lee, W. Yang, R.G. Parr, Development of the Colle–Salvetti correlation-energy formula into a functional of the electron density, Phys. Rev. B 37 (1988) 785–789.

[13] T. Yanai, D. Tew, N. Handy, A new hybrid exchange-correlation functional using the Coulomb-attenuating method (CAM-B3LYP), Chem. Phys. Lett. 393 (2004) 51–57.

[14] (a) Y. Zhao, D. Truhlar, The M06 suite of density functionals for main group thermochemistry, thermochemical kinetics, noncovalent interactions, excited states, and transition elements: two new functionals and systematic testing of four M06-class functionals and 12 other functionals, Theor. Chem. Acc. 120 (2008) 215–241;
(b) Y. Zhao, D. Truhlar, Density functionals with broad applicability in chemistry, Acc. Chem. Res. 41 (2008) 157–167.

[15] L.A. Curtiss, M.P. McGrath, J.-P. Blaudeau, N.E. Davis, R.C. Binning Jr., L. Radom, Extension of Gaussian-2 theory to molecules containing third-row atoms Ga–Kr, J. Chem. Phys. 103 (1995) 6104–6113.

[16] D. Tzeli, A. Papakondylis, A. Mavridis, J. Phys. Chem. A 102 (1998) 2223–2230.

[17] (a) J.P. Perdew, K. Burke, M. Ernzerhof, Generalized gradient approximation made simple, Phys. Rev. Lett. 77 (1996) 3865–3868;
(b) M. Enzerhof, G.E. Scuseria, Assessment of the Perdew–Burke–Ernzerhof exchange-correlation functional, J. Chem. Phys. 110 (1999) 5029–5036;
(c) C. Adamo, V. Barone, Toward reliable density functional methods without adjustable parameters: the PBE0 model, J. Chem. Phys. 110 (1999) 6158–6170.

[18] R. Improta, V. Barone, F. Santoro, Ab initio calculations of absorption spectra of large molecules in solution: Coumarin c153, Angew. Chem. Int. Ed. 46 (2007) 405–408.
[19] R. Improta, C. Ferrante, R. Bozio, V. Barone, The polarizability in solution of tetra-phenyl-porphyrin derivatives in their excited electronic states: a PCM/TD-DFT study, Phys. Chem. Chem. Phys. 11 (2009) 4664–4673.
[20] S. Miertuš, E. Scrocco, J. Tomasi, Electrostatic interaction of a solute with a continuum. A direct utilizaion of AB initio molecular potentials for the prevision of solvent effects, Chem. Phys. 55 (1981) 117–129.
[21] (a) M. Cossi, G. Scalmani, N. Rega, V. Barone, New developments in the polarizable continuum model for quantum mechanical and classical calculations on molecules in solution, J. Chem. Phys. 117 (2002) 43;
(b) J. Tomasi, B. Mennucci, R. Cammi, Quantum mechanical continuum solvation models, Chem. Rev. 105 (2005) 2999–3093;
(c) A. Pedone, J. Bloino, S. Monti, G. Prampolini, V. Barone, Absorption and emission UV–Vis spectra of the TRITC fluorophore molecule in solution: a quantum mechanical study, Phys. Chem. Chem. Phys. 12 (2010) 1000–1006.
[22] M.A .L. Marques, E.K.U. Gross, Time-dependent density functional theory, Annu. Rev. Phys. Chem. 55 (2004) 427–455.
[23] P.D. Harvey, in: K.M. Kadish, K.M. Smith, R. Guilard (Eds.), The Porphyrin Handbook: Multiporphyrins, Multiphthalocyanines and Arrays, vol. 18, Academic Press, San Diego, 2003, p. 65.
[24] (a) S.F. Boys, F. Bernardi, The calculation of small molecular interactions by the differences of separate total energies. Some procedures with reduced errors, Mol. Phys. 19 (1970) 553–566;
(b) S.S. Xantheas, On the importance of the fragment relaxation energy terms in the estimation of the basis set superposition error correction to the intermolecular interaction energy, J. Chem. Phys. 104 (1996) 8821–8825.
[25] M.J. Frisch, G.W. Trucks, H.B. Schlegel, G.E. Scuseria, M.A. Robb, J.R. Cheeseman, G. Scalmani, V. Barone, B. Mennucci, G.A. Petersson, H. Nakatsuji, M. Caricato, X. Li, H.P. Hratchian, A.F. Izmaylov, J. Bloino, G. Zheng, J.L. Sonnenberg, M. Hada, M. Ehara, K. Toyota, R. Fukuda, J. Hasegawa, M. Ishida, T. Nakajima, Y. Honda, O. Kitao, H. Nakai, T. Vreven, J.A. Montgomery, Jr., J.E. Peralta, F. Ogliaro, M. Bearpark, J.J. Heyd, E. Brothers, K.N. Kudin, V.N. Staroverov, R. Kobayashi, J. Normand, K. Raghavachari, A. Rendell, J.C. Burant, S.S. Iyengar, J. Tomasi, M. Cossi, N. Rega, J.M. Millam, M. Klene, J.E. Knox, J. B. Cross, V. Bakken, C. Adamo, J. Jaramillo, R. Gomperts, R.E. Stratmann, O. Yazyev, A.J. Austin, R. Cammi, C. Pomelli, J.W. Ochterski, R.L. Martin, K. Morokuma, V.G. Zakrzewski, G.A. Voth, P. Salvador, J.J. Dannenberg, S. Dapprich, A.D. Daniels, O. Farkas, J.B. Foresman, J.V. Ortiz, J. Cioslowski, D.J. Fox, Gaussian 09, Revision A.1, Ga ussian, Inc., Wallingford CT, 2009.
[26] (a) A. Gebauer, D.Y. Dawson, J. Arnold, Synthesis and characterization of a neutral Li-porphyrin radical, J. Chem. Soc. Dalton Trans. (2000) 111–112;
(b) L.-C. Xu, Z.-Y. Li, T.-J. He, F.-C. Liu, D.-M. Chen, Density functional theory studies of lithium porphyrin radicals, Chem. Phys. 305 (2004) 165–174.
[27] (a) S. Ishikawa, G. Madjarova, T.J. Yamabe, First-principles study of the lithium interaction with polycyclic aromatic hydrocarbons, Phys. Chem. B 105 (2001) 11986–11993;
(b) C.F. Guerra, J.-W. Handgraaf, E.J. Baerends, F.M. Bickelhaupt, Voronoi Deformation Density (VDD) charges. Assessment of the Mulliken, Bader, Hirshfeld, Weinhold and VDD methods for Charge Analysis, J. Comput. Chem. 25 (2004) 189–210.
[28] M. Gouterman, Study of the effects of substitution on the absorption spectra of porphin, Mater. J. Chem. Phys. 30 (1959) 1139–1161.
[29] X. Huang, K. Nakanishi, N. Berova, Porphyrins and metalloporphyrins: versatile circular dichroic reporter groups for structural studies, Chirality 12 (2000) 237–255.
[30] J. Mack, M. Stillman, Assignment of the optical spectra of metal phthalocyanines through spectral band deconvolution analysis and ZINDO calculations, J. Coord. Chem. Rev. 219–221 (2001) 993–1032.